A&A 474, L21–L24 (2007)
DOI: 10.1051/0004-6361:20078362

Astronomy & Astrophysics

Letter to the Editor

K–H_2 quasi-molecular absorption detected in the T-dwarf ε Indi Ba

F. Allard[1,2], N. F. Allard[2,3], D. Homeier[4], J. Kielkopf[5], M. J. McCaughrean[6], and F. Spiegelman[7]

[1] Centre de Recherche Astrophysique de Lyon, UMR 5574: CNRS, Université de Lyon, École Normale Supérieure de Lyon, 46 allée d'Italie, 69364 Lyon Cedex 07, France
e-mail: fallard@ens-lyon.fr
[2] Institut d'Astrophysique de Paris, UMR 7095: CNRS, Université Pierre et Marie Curie-Paris 6, 98bis boulevard Arago, 75014 Paris, France
[3] Observatoire de Paris-Meudon, LERMA, UMR 8112, CNRS, 92195 Meudon Principal Cedex, France
[4] Institut für Astrophysik, Georg-August-Universität, Friedrich-Hund-Platz 1, 37077 Göttingen, Germany
[5] Department of Physics and Astronomy, University of Louisville, Louisville, KY 40292, USA
[6] School of Physics, University of Exeter, Stocker Road, Exeter EX4 4QL, UK
[7] Laboratoire de Chimie et Physique Quantiques, UMR5626, CNRS and Université Paul Sabatier, 118 route de Narbonne 31062, Toulouse Cedex, France

Received 27 July 2007 / Accepted 27 August 2007

ABSTRACT

Context. T-type dwarfs present a broad and shallow absorption feature centred around 6950 Å in the blue wing of the K doublet at 0.77 μm which resembles in depth and shape the satellite absorption predicted by detailed collisional broadening profiles. In our previous work, the position of the predicted line satellite was however somewhat too blue compared to the observed feature.
Aims. In this paper, we investigate whether new calculations of the energy surfaces of the potentials in the K–H_2 system, including spin-orbit coupling, result in a closer coincidence of the satellite with the observed position. We also investigate the extent to which CaH absorption bands contribute to the feature and at what $T_{\rm eff}$ these respective opacity sources predominate.
Methods. We present model atmospheres and synthetic spectra, including gravitational settling for an improved description of depth-dependent abundances of refractory elements, and based on new K–H_2 line profiles using improved interaction potentials.
Results. By comparison with a high signal-to-noise optical spectrum of the T1 dwarf ε Indi Ba, we find that these new models do reproduce the observed feature, while CaH does not contribute for the atmospheric parameters considered. We also find that CaH is settled out so deep into the atmosphere that even turbulent vertical mixing would appear insufficient to bring significant amounts of CaH to the observable photosphere in dwarfs of later type than ~L5.
Conclusions. We conclude that previous identification of the feature at this location in the spectra of T dwarfs as well as the latest L dwarfs with CaH was erroneous, as expected on physical grounds: calcium has already condensed onto grains in early L dwarfs and thus should have settled out of the photosphere in cooler brown dwarfs. This finding revokes one of the observational verifications for the cloud-clearing theory assumption: a gradual clearing of the cloud cover in early T dwarfs.

Key words. stars: low-mass, brown dwarfs – stars: atmospheres – line: profiles

1. Introduction

Late L- and T-type brown dwarfs have atmospheres composed primarily of molecular hydrogen and helium. Most refractory metals condense out to grains in previous evolutionary phases (early L type) and should settle below their fully radiative upper photospheres. Alkali elements bind less readily to molecules or grains and their resonance transitions remain the last sources of opacity at optical wavelengths, along with Rayleigh scattering by H_2 and He. Alkali line broadening therefore defines the local "continuum" out to several thousands of Ångströms from the line cores of the neutral K and Na D doublets at 0.59 and 0.77 μm, respectively. Burrows & Volobuyev (2003, and references therein) have shown that these far wings deviate greatly from the simple Lorentzian shape, and speculated on the existence of *satellite features* in the blue wings due to a local extremum in the energy shift.

A number of T dwarfs show an absorption feature at 6950 Å which Burgasser et al. (2003) identified as a CaH band. This was a somewhat curious suggestion, however, because calcium condenses onto grains in L dwarfs already and is thus expected to have settled out of the photosphere of cooler brown dwarfs. The identification of this feature with CaH (as well as the observation of FeH bands) led to believe that it was a proof for vertical mixing and clearing of the cloud cover in T dwarfs (Burgasser et al. 2003).

As alternative, we propose that the feature should rather be identified with quasi-molecular absorption by K–H_2. Allard et al. (2003b) calculated absorption profiles of the K doublet at 0.77 μm for H_2 and He perturbers, based upon the K–H_2 and K–He interaction potentials calculated by Rossi & Pascale (1985, hereafter RP85) and Pascale (1983, hereafter P83) using a semi-classical approach. The resulting models and synthetic spectra revealed a K–H_2 satellite feature with similar depth and width to that observed at 6950 Å in the T dwarfs, but at a shorter wavelength of 6830 Å. In this paper, we present new models based on line profiles for K–H_2 calculated with updated potentials (see Allard et al. 2007a, hereafter S06).

2. Model atmospheres

We have used the stellar atmosphere code PHOENIX (Hauschildt & Baron 1999) version 15. With respect to previous versions used by Allard et al. (2001) to determine the limiting effects of dust grain formation of the atmospheres of low-mass stars and brown dwarfs, the chemical equilibrium (CE) code in this version has been modified to include grain settling effects (Allard et al. 2007c). For each layer of the model atmosphere, atarting at the deepest cloud condensation layer (as set by the CE calculation), dust grain number densities are calculated in equilibrium to the gas phase. Condensation, gravitational settling and turbulence mixing timescale are compared to predict the fraction of grains which must settle (see also Allard et al. 2003a). This grain fraction is then removed from the composition and a new equilibrium is obtained. This process is repeated until the grain density no longer changes. The advantage of this method compared to an a priori reduction of refractory elemental abundances is an automatic depletion of the elemental abundances as a function of temperature and pressure, in the sequence of formation of the diverse grain types. For example, Zr will be depleted first from the gas phase, as ZrO_2 is the grain that forms at the highest temperature, followed at lower temperatures by Fe, Mg ($MgSiO_3$), Al (Al_2O_3), and so on. The Allard et al. (2001) "Cond" models – which used an equilibrium dust distribution but simulated gravitational settling by commenting out dust opacities – tended to retain some trace of the molecular compounds involved in the grains. Here the depletion is complete and, for example, no TiO absorption band opacity remains in layers where grains involving Ti have been found to condense. This formalism corresponds therefore to a more accurate description of grain settling.

In the Settl models described above, gravitational settling efficiently clears the uppermost region of the photosphere from dust down to a few pressure scale heights from the top of the convection zone. A full description of these models exceeds the scope of this paper and will be published separately.

3. New line profiles

An important improvement with respect to the 2001 Cond models is the inclusion of the pressure broadening profiles for the neutral alkali resonance lines of Li I by Allard et al. (2005), Rb I and Cs I by Allard & Spiegelman (2006), K I and Na I D as in Allard et al. (2003b) and by Allard et al. (2007a). These profiles include fine structure and use damping constants for the Lorentz line cores from semi-classical theory (Allard et al. 2007b).

The most important contributions to the satellite feature under consideration come from H_2 and He. The profiles of K-H_2 account for two different orientations of the H_2 molecule: C_{2v}, where the H_2 molecular axis is perpendicular to the K radiating atom, and $C_{\infty v}$, where all atoms are collinear. The C_{2v} S06 satellite is predicted to lie at 6980 Å, while the weaker $C_{\infty v}$ contribution peaks at 6920 Å: these should be compared to 6851 and 6695 Å, respectively, for the RP85 profiles. The K–He satellite is predicted to be at 6930 Å. Note, however, that when accounting for intermediate orientations of the H_2 molecule, additional satellite contributions may wash out and slightly change the predicted position. Santra & Kirby (2005) have published ab initio potentials for K–H_2 at 4 orientations of the H_2 molecule, as well as for K-He, predicting K–H_2 satellites around 6920 Å and 6850 Å for the C_{2v} and $C_{\infty v}$ orientations, respectively, with K–He at 7000 Å. These values correspond to the extrema of the difference potentials, however: our corresponding values are 6906 Å and 6830 Å for C_{2v} and $C_{\infty v}$, respectively. Finally, Zhu et al. (2006) have also computed profiles of K and Na perturbed by He, finding a K-He satellite at 7080 Å. Combined, these calculations predict a broad absorption feature with properties very similar to that observed at 6850 to 7100 Å and centred at 6950 Å) in the spectra of T dwarfs such as ε Indi Ba as discussed below.

4. Optical spectral analysis of the T1 dwarf ε Indi Ba

The ε Indi Ba,b binary system is a unique test for brown dwarf models. They are the closest known brown dwarfs to the Sun, allowing spectra to be obtained with high signal-to-noise in the faint optical range. The well-determined HIPPARCOS distance (3.626 pc) allows accurate comparison to be made with models at an absolute level. Based on their *JHK* photometry and *H*-band spectra, McCaughrean et al. (2004) obtained effective temperatures of 1276 K and 854 K for Ba and Bb, respectively, using the Baraffe et al. (2003) 1.3 Gyr Cond isochrone for the most likely age of the ε Indi AB system. This corresponds to surface gravities of $\log g = 5.15$ and 4.9, and radii of 0.091 and 0.096 $R_\odot$, respectively. We have compared a Settl model calculated for these parameters to a medium-resolution resolved optical spectrum of the T1 primary (Ba), as shown in Fig. 1.

As part of a comprehensive 0.6–5 μm photometric and spectroscopic study of ε Indi Ba,b, the ESO VLT was used on June 16 2004 to obtain optical (0.6–0.86 μm) spectroscopy using FORS2 in long-slit mode, with a slit width of 0.5 arcsec and the HR collimator. In this mode, the 600RI grism yielded a spectral resolution of $R \sim 1000$ at 6780 Å, while the seeing of 0.35 arcsec FWHM ensured that the two T dwarfs, separated by ~0.8 arcsec at that epoch, were well-resolved spatially. A total integration time of 80 min was obtained by co-adding 6×800 s individual exposures. The data reduction was standard, using skylines for wavelength calibration, dome lights for spectral flat-fielding, and the DC white dwarf spectrophotometric standard, LTT 9491, for flux calibration. Unfortunately, no direct telluric calibration was possible, but an excellent cancellation of all known telluric features was achieved by using the NSO Kitt Peak atmospheric transmission spectrum (Hinkle et al. 2003) convolved to the FORS2 resolution and with iterative adjustment of the effective airmass to match the conditions over Paranal at the time of our observations. This allowed efficient removal of the 6884 Å O_2 B band close to the satellite (compare Fig. 2). Further details of the data reduction will be given by King et al. (2007, in prep). Preliminary absolute flux calibration was obtained by using the combined *I*-band photometry from the DENIS second data release[1], as listed in McCaughrean et al. (2004), to calibrate a composite spectrum of ε Indi Ba,b taken with the EFOSC spectrograph at the ESO 3.6 m telescope, the red part of which is also shown in Fig. 1. The FORS2 spectrum was then rescaled to match the composite spectrum at $\lambda < 8000$ Å, where the flux contribution of the Bb component is less than 1%.

Our synthetic spectrum reproduces the near-IR photometry for Ba to within 0.15 mag, supporting our treatment of dust opacity, which shapes the infrared SED in transition objects. The red optical region is extremely well reproduced in most details, including the shape of the K doublet at 0.77 μm and the depth of the secondary alkali lines of Rb I and Cs I, absorbing through the red wing of the K I doublet. Assuming a meteoritic, i.e. proto-solar, lithium abundance, the model also predicts a strong Li I 6707 Å doublet, but this is not observed. This implies a relatively massive object which depleted its Li at a young age when

[1] http://vizier.u-strasbg.fr/viz-bin/Cat?B/denis

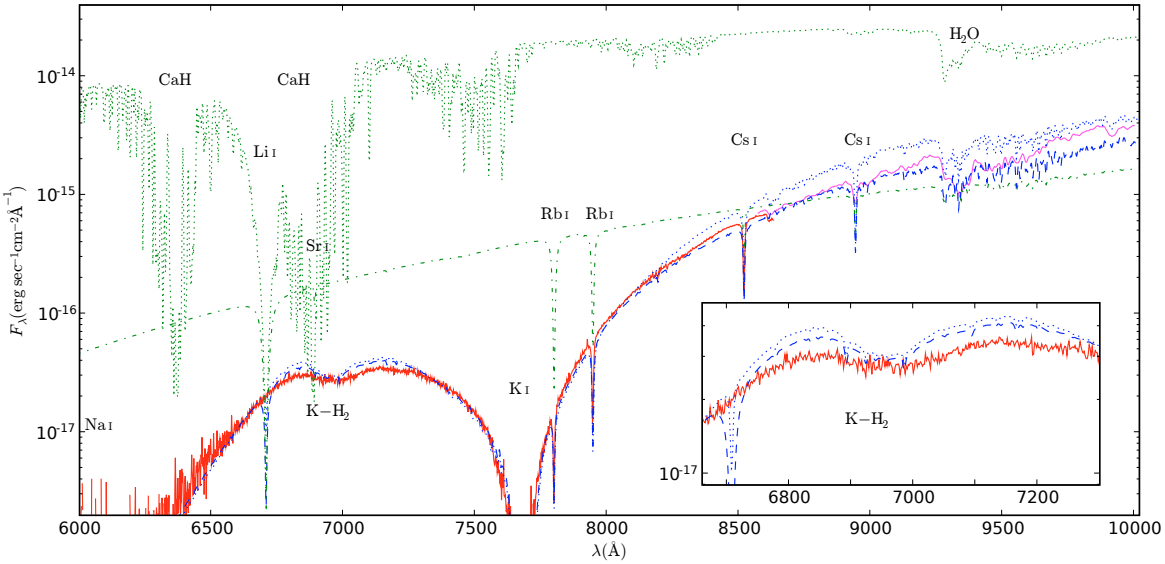

Fig. 1. FORS2 red optical spectrum of the T1 dwarf ε Indi Ba (solid), compared to our synthetic spectra for a 1.3 Gyr (dashed) and 2 Gyr (dotted) model. To highlight the various sources of opacity, spectra obtained when the K and Na D doublets are omitted (dot-dashed), and when dust grains involving Ca and other refractory species are prevented from forming and raining out (upper dotted line) are also shown. All molecular bands but CaH and H_2O have been omitted from the latter spectrum for clarity. The EFOSC spectrum of ε Indi Ba,b is shown from 8600–10 000 Å (light [magenta] solid line) against a composite model of both T dwarfs.

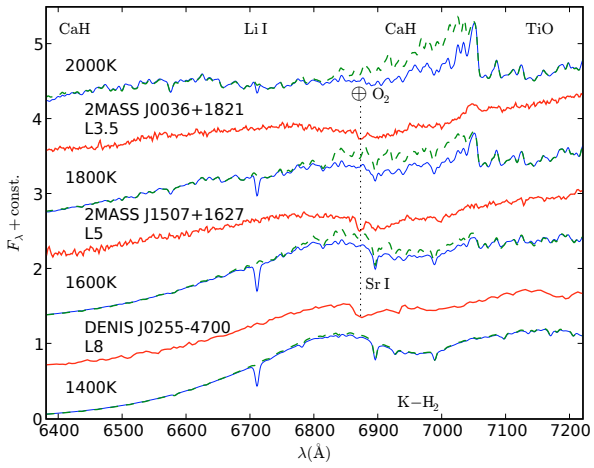

Fig. 2. Effective temperature sequence of $\log g = 5.0$ Settl models with (solid) and without (dashed) CaH band opacity. The synthetic spectra have been degraded to 5 Å resolution for comparison with L dwarf spectra (thick [red] lines) observed with the Keck LRIS spectrograph (Reid et al. 2001, 2000; Martín et al. 1999). Spectral subtypes of the L dwarfs are given in the optical classification system of Kirkpatrick et al. (1999, in prep.[2]); note that DENIS J 0255−4700 has been typed L6 in the system of Martín et al. (1999). The sharp CaH band head near 7075 Å vanishes in both observed and model spectra between about L5 and L8, and a distinctive absorption feature emerges that extends well to the red of the original CaH band head. The models have Li abundance reduced to 1% (solid) and 0.1% (dashed), indicating strong Li depletion in all these field L dwarfs.

its atmosphere was fully convective and its core temperature exceeded the Li burning threshold: this process consumes most Li in brown dwarfs more massive than 0.055–0.06 $M_\odot$ in the first Gyr of their lifetime (Zapatero Osorio et al. 2005).

According to the Baraffe et al. (2003) evolutionary tracks, a 0.055 $M_\odot$ brown dwarf at an age of 2.0 Gyr should have $T_{\rm eff}$ = 1350 K, $\log g$ = 5.30 and R = 0.086 $R_\odot$. This model is overplotted as dotted line in Fig. 1 and still agrees with the data within observational and modelling uncertainties. For a qualitative estimate of the degree of lithium depletion we have reduced the elemental Li abundance in this latter model by 1.5 dex. It still shows a clearly visible resonance line not detectable in the observation, confirming very low Li abundance.

The models also show a weak 6894.5 Å Sr I line against the background of the alkali lines. It is not detectable in the observed spectrum, indicating incomplete treatment of Sr condensation.

4.1. The K–H_2 satellite

The key feature in this high signal-to-noise spectrum for present purposes is the shallow absorption feature centred at 6950 Å, the exact location of the satellite of the K–H_2 interaction with the 0.77 μm doublet as newly predicted here using the S06 profiles (Figs. 1 and 2). However, the new satellite apparently extends not far enough to the red to reproduce the more elongated shape of the observed feature. K–He produces a satellite which might reproduce the observed extent of the feature to 7100 Å according to the Santra & Kirby (2005) and Zhu et al. (2006) calculations. Our old potentials predict it further to the blue, from 6930−6980 Å, thus superimposing on the location of the K–H_2 satellite and producing an absorption trough that is too narrow.

4.2. The CaH $A^2\pi$–$X^2\Sigma$ band

The dot-dashed line in Fig. 1 shows the effect of eliminating the large wings of the K and Na D doublet, to reveal other opacity sources which participate in the formation of the spectrum. The Settl model does not predict any features besides the Sr I line (compare also Fig. 2) in the spectral region of the satellite.

However, if we artificially prevent calcium from being locked into grains and settled out, the $A^2\pi - X^2\Sigma$ band of CaH is seen, partly coincident with the observed feature (upper

[2] See http://DwarfArchives.org

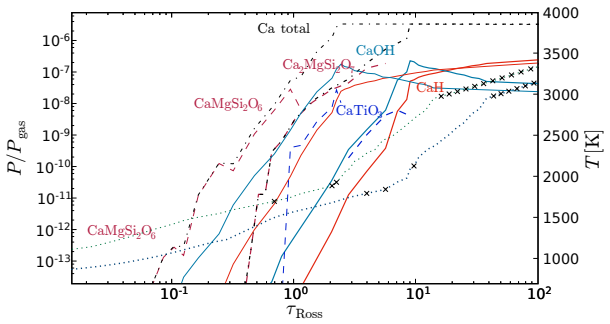

Fig. 3. Partial pressures of principal Ca-bearing species versus optical depth in the Settl model for $T_{\rm eff}$ = 1280 K (thick lines) and 1600 K (thin lines). Gas temperature is shown (dotted lines) with the convection zones indicated (crosses), right scale.

dotted line in Fig. 1). This led Burgasser et al. (2003) to propose that CaH is responsible for the observed feature in early to mid-T dwarfs, advocating a possible resurgence of CaH due to upwelling of CaH or cloud-clearing effects.

We find that most calcium is locked into diopside ($CaMgSi_2O_6$) and akermanite ($Ca_2MgSi_2O_7$) below 1900 K, leading to a depletion of calcium to 10^{-4} or less as these condensates settle out (Fig. 3). CaH only prevails at solar abundances deep in the optically-thick atmosphere, independent of whether we account for clouds or not.

Figure 2 illustrates the difference between models with and without CaH bands for effective temperatures ranging across the late-L sequence. At 2000 K, the CaH band does indeed shape the pseudo-continuum at 6800–7050 Å, but by 1600 K, the K–H_2 satellite is dominant and CaH barely contributes to the absorption. While the intensity of the satellite actually increases with gas temperature (see Figs. 10−12 of S06), in our model spectra the satellite grows in strength with *decreasing* $T_{\rm eff}$, due to clearing of the atmosphere and increased pressure in the line-forming region (see Allard et al. 2007c, for details). It creates an absorption trough extending from 6850 to 7100 Å, visible in the observed spectra of the late L dwarfs, where it is extending beyond the CaH band head and even further to the red than in the models (cf. Sect. 4.1). Once T dwarf temperatures are reached, our models retain essentially no CaH opacity, challenging the cloud-clearing picture unless condensable gas is upwelled efficiently over more than two pressure scale-heights by turbulence.

5. Summary

We have computed new model atmospheres based on detailed absorption profiles for the neutral Na D, Li, K, Rb, and Cs alkali lines (RP85 and P83 potentials) and, in particular, new interaction potentials (S06) for K–H_2. These new models predict a K–H_2 satellite absorption feature at 6950 Å closely matching the position and shape of an observed feature in the spectrum of the T1 dwarf ε Indi Ba. We therefore conclude that the K–H_2 satellite is the most natural explanation for the feature, rather than CaH as has been previously proposed. Indeed, the high (solar) abundance of CaH which would be required to generate absorption near this spectral location should only be found deep in the optically-thick atmosphere at the $T_{\rm eff}$ = 1280 K of ε Indi Ba, preventing its bands from appearing in spectra even assuming a clearing of the surface cloud coverage.

Acknowledgements. Part of this work was financially supported by the PNPS program of the CNRS and the EC MC RTN CONSTELLATION (MRTN–CT–2006–035890). We also thank the CINES, IDRIS, and the GWDG for generous allocations of computing time necessary to complete this project, and an anonymous referee for valuable comments on the manuscript. NFA is grateful to A. Staiano for his help in computing K–H_2 opacity tables and DH to Sandy Leggett for electronic versions of the LRIS spectra. This work has also benefited from the M, L, and T dwarf compendium housed at `DwarfArchives.org` and maintained by Chris Gelino, Davy Kirkpatrick, and Adam Burgasser, and from the IAC ultracool dwarf catalogue at `http://www.iac.es/galeria/ege/catalogo_espectral` compiled by Juan Cabrera and Elena Cenizo under the direction of Eduardo Martín.

References

Allard, N. F., & Spiegelman, F. 2006, A&A, 452, 351
Allard, F., Hauschildt, P. H., Alexander, D. R., Tamanai, A. & Schweitzer, A. 2001, ApJ, 556, 357
Allard, F., Guillot, T., Ludwig, H.-G., et al. 2003a, in Brown Dwarfs, ed. E. Martín (San Francisco: ASP), IAU Symp., 211, 325
Allard, N. F., Allard, F., Hauschildt, P. H., Kielkopf, J. F., & Machin, L. 2003b, A&A, 411, L473
Allard, N. F., Allard, F., & Kielkopf, J. F. 2005, A&A, 440, 1195
Allard, N. F., Spiegelman, F., & Kielkopf, J. K. 2007a, A&A, 465, 1085 (S06)
Allard, N. F., Kielkopf, J. F., & Allard, F. 2007b, EPJD, accepted
Allard, F., Homeier, D., Guillot, T., et al. 2007c, A&A, in prep.
Baraffe, I., Chabrier, G., Barman, T. S., Allard, F., & Hauschildt, P. H. 2003, A&A, 402, 701
Burgasser, A. J., Kirkpatrick, J. D., Liebert, J., & Burrows, A. 2003, ApJ, 594, 510
Burrows, A., & Volobuyev, M. 2003, ApJ, 583, 985
Hauschildt, P. H., & Baron, E. 1999, J. Comput. Appl. Math., 109, 41
Hinkle, K. H., Wallace, L., & Livingston, W. 2003, Bull. AAS, 35, 1260
Kirkpatrick, J. D., Reid, I. N., Liebert, J., et al. 1999, ApJ, 519, 802
Martín, E. L., Delfosse, X., Basri, G., et al. 1999, AJ, 118, 2466
McCaughrean, M. J., Close, L. M., Scholz, R.-D., et al. 2004, A&A, 413, 1029
Pascale, J. 1983, Phys. Rev. A, 28, 632 (P83)
Reid, I. N., Kirkpatrick, J. D., Gizis, J. E., et al. 2000, AJ, 119, 369
Reid, I. N., Burgasser, A. J., Cruz, K. L., Kirkpatrick, J. D., & Gizis, J. E. 2001, AJ, 121, 1710
Rossi, F., & Pascale, J. 1985, Phys. Rev. A, 32, 2657 (RP85)
Santra, R., & Kirby, K. 2005, J. Chem. Phys., 123, 214309
Zapatero Osorio, M. R., Martín, E. L., Lane, B. F., et al. 2005, AN, 326, 948
Zhu, C., Babb, J. F., & Dalgarno, A. 2006, Phys. Rev. A, 73, 012506